PHYSICAL REVIEW B VOLUME 43, NUMBER 4 1 FEBRUARY 1991

Numerical computation of the flux-line-lattice structure of an inhomogeneous material in the London approximation

L. L. Daemen and J. E. Gubernatis
Theoretical Division, Los Alamos National Laboratory, Los Alamos, New Mexico 87545
(Received 7 September 1990)

We present the basic equations that permit the efficient simulation of vortex structures in inhomogeneous materials whose superconducting behavior is described by the London equations. In analogy to homogeneous materials, we show that the energy of such structures is the sum of a self-interaction part, which depends on the local variation of the penetration depth, and a sum of pair interactions, which are the Green's functions of the London equation for an inhomogeneous material. This formalism permits simulations in which the exact, long-range London interactions between flux lines are used. In addition, the realistic modeling of defects by allowing the penetration depth to vary spatially is possible, and pinning, instead of being assumed, arises in a natural manner by local variations in Lorentz forces. The equations were solved for a variety of one-dimensional models of inhomogeneities, and physically reasonable flux-line lattices were found. A suggestion for the use of the formalism to study the dynamic properties of flux-line lattices is made.

I. INTRODUCTION

Most static and dynamic macroscopic magnetic properties of type-II superconductors are determined by the flux-line lattice (FLL). These properties, in turn, intimately depend on the material. Microstructural defects (inhomogeneities) interact with the flux lines and create the pinning forces acting on the vortices. These forces, together with the intervortex interactions and thermal fluctuations, determine the static and dynamic properties of the FLL. Consequently, it is of interest, particularly for static properties, to understand how the FLL structure is affected by different types of microstructural defects such as grain boundaries, twinning planes, normal-state inclusions, voids, etc. However, because these defects are often randomly distributed, the background potential in which a flux lines moves is, in general, quite complex. This complexity makes a detailed, analytic resolution of the equation of motion for the FLL possible only for restricted simplified, geometries.[1-3] Hence, for potentially more realistic microstructures, a numerical approach is necessary.

Brandt[4] was the first to simulate numerically the interaction of vortices with pinning centers. He assumed that the vortex lattice energy could be written as a sum of pairwise interactions between vortices plus a sum of interactions between the vortices and postulated pinning centers. He simplified the problem by considering a set of pointlike vortices interacting among themselves via a short-range, Gaussian-like potential, and interacting with fixed, attractive, randomly distributed, pinning centers also described by a Gaussian-like potential. The choice of Gaussian interactions was made solely for computational convenience. With this modeling, he calculated minimum-energy vortex configurations for a variety of pinning center configurations and various vortex and pinning center densities. He focused on the elastic and plastic properties of the FLL as well as estimates of critical pinning forces and currents.

In a series of papers, Jensen and co-workers[5] studied numerically the onset of diffusion in the FLL in a thin-film superconductor. Using modeling similar to that of Brandt, these authors were also mainly concerned with the elastic properties of the FLL, and by using a combination of molecular dynamics and annealing techniques, they integrated numerically the equation of motion for a flux line, calculated the elastic properties of the FLL, simulated flux flow, and determined such macroscopic properties as voltage-current characteristics.

The above heuristic modeling of the interactions is in sharp contrast to what is possible for a homogeneous material. For vortices with pointlike cores, the London equation is appropriate. From this equation the interaction between vortices (for an infinite material) is easily found in terms of an analytic solution. The energy of the system consists of two parts: one part is the self-energy of a vortex while the other is a pairwise sum of the interactions between vortices. Since the self-energy for a homogeneous system is independent of vortex position, only the "two-body" interaction contributes to the FLL. With this interaction, the energies of different, regular lattice structures are easily calculated and compared to determine which represents the lowest-energy configuration. The lattice is "pinned" since the Lorentz force acting at each vortex core is zero.

In this paper, we restrict ourselves to studying FLL structures in the presence of different inhomogeneities. We will proceed in a manner analogous to the study of homogeneous materials. We will demonstrate that even in the presence of inhomogeneities the energy of a system of vortices is the sum of self-energy and of pairwise interaction contributions. The pairwise interaction is a solution of London's equation, which, in general, can be found only by solving this equation numerically. Since

 ©1991 The American Physical Society

the disorder, which is introduced through a spatially varying penetration depth $\lambda(\mathbf{r})$, will in general prohibit regular lattices from being formed, we will find the proper FLL by minimizing numerically the energy of the system by adjusting the vortex core positions. Since the interaction is not a function of distance between vortex pairs, but will depend on absolute positions, this will require a constant recomputation of the interactions until the minimum-energy configuration is reached. Thus, in contrast to the above papers, to determine the FLL, we will use the correct, long-ranged interaction between the vortices. Pinning sites are not assumed, but will develop naturally as a consequence of the Lorentz force acting on the vortex caused by the inhomogeneities locally disrupting the magnetic fields surrounding the current carrying vortex cores.

Our main intent is to present a "proof of concept." Although we will present our basic equations for a two-dimensional geometry, we will, for computational expediency, restrict our calculations to one dimension. Even so, we find many physically interesting results: The vortices are, in general, repelled by regions of low penetration depth and attracted to regions of high penetration depth. The number of vortices occupying a high λ region can saturate, at which point the region begins to act as a repulsive one.

The rest of the paper is organized as follows. Section II describes the model used to determine the FLL structure and Sec. III details our numerical technique. In Sec. IV, we report our results for a simple one-dimensional case. In the last section, we state our conclusions and discuss plans for two-dimensional simulations of related problems.

II. MODEL SYSTEM

We consider a two-dimensional superconductor in the London approximation, where the coherence length $\xi \to 0$. In this approximation, the vortices are treated as pointlike objects. This approximation is expected to be justified for the new high-T_c superconductors because of their large penetration depth λ and short coherence length ξ. The problem consists of finding the spatial configuration of a set of interacting vortices in the presence of various defects. This configuration is the one that minimizes the total energy of the system, so our task is first to obtain a general expression for the free energy of a system of vortices and then to minimize it with respect to vortex positions.

A general, analytic expression for the free energy can be obtained in terms of the Green's function of the London equation with a spatially varying λ. The derivation follows de Gennes' for a position-independent λ material,[6] and generalizes his result. We start by considering a set of N interacting flux lines in a two-dimensional superconductor, where the penetration depth is an arbitrary function of position. In the London approximation, the magnetic-field distribution of a single isolated vortex line at $\mathbf{r}'$ is the solution of the equation:[3]

$$\nabla\times[\lambda^2(\mathbf{r})\nabla\times\mathbf{b}(\mathbf{r},\mathbf{r}')]+\mathbf{b}(\mathbf{r},\mathbf{r}') = \Phi_0\delta(x-x')\delta(y-y')\hat{z} , \quad (1)$$

where Φ_0 is the flux quantum and $\mathbf{b}(\mathbf{r},\mathbf{r}')$ is the magnetic field at $\mathbf{r}$ set up by a vortex at $\mathbf{r}'$. Since this equation is linear in $\mathbf{b}(\mathbf{r},\mathbf{r}')$, the total field $\mathbf{B}(\mathbf{r})$ in the presence of N flux lines can be written as a linear superposition of the field of the individual flux lines:

$$\mathbf{B}(\mathbf{r})=\sum_{i=1}^{N}\mathbf{b}(\mathbf{r},\mathbf{r}_i) , \quad (2)$$

where $\mathbf{r}_i$ designates the position of the ith flux line. The reciprocity $\mathbf{b}(\mathbf{r},\mathbf{r}')=\mathbf{b}(\mathbf{r}',\mathbf{r})$, characteristic of a Green's function, also holds. The total energy of the system is given by

$$E=\frac{1}{2\mu_0}\int d^3r[B^2(\mathbf{r})+\lambda^2(\mathbf{r})|\nabla\times\mathbf{B}(\mathbf{r})|^2] . \quad (3)$$

$E=E(\mathbf{r}_1,\mathbf{r}_2,\ldots,\mathbf{r}_N)$ is a nonlinear function of the positions of the N flux lines. Using elementary vector algebra, we can rewrite E as

$$E=\frac{1}{2\mu_0}\int\int_S\lambda^2(\mathbf{r})\{\mathbf{B}(\mathbf{r})\times[\nabla\times\mathbf{B}(\mathbf{r})]\}\cdot d\boldsymbol{\sigma}$$

$$=\frac{1}{2\mu_0}\sum_{i=1}^{N}\int\int_{\sigma_i}\lambda^2(\mathbf{r})\{\mathbf{B}(\mathbf{r})\times[\nabla\times\mathbf{B}(\mathbf{r})]\}\cdot d\boldsymbol{\sigma} . \quad (4)$$

where S designates the set of cylindrical surfaces σ_i, of arbitrary radius ξ centered at the center of each vortex core. Equation (4) is the same as that obtained in the special case when λ is position independent. Upon substituting Eq. (2) into Eq. (4) and using the same procedures as de Gennes[6] to simplify the resulting expression, we can rewrite the total energy of a system of interacting flux lines as a sum of one-body and two-body terms:

$$E=\frac{1}{2\mu_0}\sum_{i=1}^{N}\int\int_{\sigma_i}\lambda^2(\mathbf{r})\{\mathbf{b}(\mathbf{r},\mathbf{r}_i)\times[\nabla\times\mathbf{b}(\mathbf{r},\mathbf{r}_i)]\}\cdot d\boldsymbol{\sigma}$$

$$+\frac{1}{\mu_0}\sum_{i<j}^{N}\int\int_{\sigma_i}\lambda^2(\mathbf{r})\{b(\mathbf{r},\mathbf{r}_j)\times[\nabla\times\mathbf{b}(\mathbf{r},\mathbf{r}_i)]\}\cdot d\boldsymbol{\sigma}$$

$$\equiv E_1+E_2 . \quad (5)$$

The two-body interaction term can be simplified further. We first consider the term in the double sum (6) and let $\mathbf{r}'=\mathbf{r}-\mathbf{r}_i$:

$$e_{ij}=\frac{1}{\mu_0}\int\int_{\sigma_i}\lambda^2(\mathbf{r}'+\mathbf{r}_i)\{\mathbf{b}(\mathbf{r}'+\mathbf{r}_i,\mathbf{r}_j)\times[\nabla_{\mathbf{r}'}\times\mathbf{b}(\mathbf{r}',\mathbf{r}_i)]\}\cdot d\boldsymbol{\sigma}_i . \quad (6)$$

Upon expressing the integrand in cylindrical coordinates (r',ϕ,z), and using $\mathbf{b}=b_z(r',\phi)\hat{\mathbf{e}}_z$, we find that

$$e_{ij}=\frac{1}{\mu_0}\int_0^{2\pi}d\phi\,\xi\lambda^2(\mathbf{r}'+\mathbf{r}_i)\mathbf{b}(\mathbf{r}'+\mathbf{r}_i,\mathbf{r}_j)\frac{\partial b_z}{\partial r'}(\mathbf{r}',\mathbf{r}_i) , \quad (7)$$

where e_{ij} is now the energy per unit length of the flux line. If we take the limit $\xi\to 0$ and exchange the summation and limit, we get

$$e_{ij}=\frac{1}{\mu_0}2\pi\lambda^2(\mathbf{r}_i)b_z(\mathbf{r}_i,\mathbf{r}_j)\lim_{\xi\to 0}\left[\xi\frac{\partial b_z}{\partial r'}\bigg|_{r'=\xi}\right] . \quad (8)$$

For $r' \to 0$ and for sufficiently small ξ, one must recover the homogeneous result for b_z, namely

$$b_z(r', \mathbf{r}_i) = \frac{\Phi_0}{2\pi\lambda^2(\mathbf{r}_i)} K_0 \left[\frac{r'}{\lambda^2(\mathbf{r}_i)} \right] . \tag{9}$$

Then, using the behavior of the modified Bessel function for small arguments, $K_0(x) \sim -\ln x$, it is easy to show that the limit appearing in (8) equals $\Phi_0/2\pi\lambda^2(\mathbf{r}_i)$. So, we can reduce (6) to the remarkably simple result:

$$E_2 = \frac{\Phi_0}{\mu_0} \sum_{i<j}^{N} b_z(\mathbf{r}_i, \mathbf{r}_j) . \tag{10}$$

To obtain Eq. (10), we used the reciprocity property of the Green's function, $b_z(\mathbf{r}_i, \mathbf{r}_j) = b_z(\mathbf{r}_j, \mathbf{r}_i)$.

The one-body term E_1 in Eq. (6) is somewhat more delicate to manipulate. In the limit that $\xi \to 0$, this term diverges logarithmically. It represents the self-energy of the flux line and is position dependent if the penetration depth is position dependent. A finite cutoff ξ has to be chosen to keep it finite. In what follows, we will set ξ equal to the coherence length of the superconductor and write

$$E_1 = \frac{\Phi_0}{2\pi\mu_0} \sum_i \frac{1}{\lambda(\mathbf{r}_i)^2} . \tag{11}$$

One can already see that the structure of the FLL will be determined solely by the competition between the one-body and the two-body terms in E. The one-body term will tend to move a vortex to a region of the sample where the penetration depth λ is large to minimize the vortex self-energy. This tendency will be counterbalanced by the repulsive force between the flux lines described by the two-body term, which will prevent the vortices from clustering at one location in the superconductor.

An important aspect of the problem consists in choosing the spatially varying penetration depth $\lambda(\mathbf{r})$ to model more or less accurately actual defects and inhomogeneities. It should be emphasized that there are essentially two different types of pinning mechanisms.[7] Core pinning results from the interaction between the normal vortex core and a local inhomogeneity. The condensation energy required to make the order parameter equal to zero at the center of a vortex core can be recovered if the vortex sits in a region of the material where the order parameter is already zero, or is smaller than its normal value. Magnetic pinning results from various large scale inhomogeneities, such as a large void, a planar boundary, or an inclusion, that distort the supercurrent configuration in the vicinity of a vortex. This distortion causes a nonzero current to exist at a vortex core and hence, induces a Lorentz force acting on the vortex. A number of large scale defects and inhomogeneities can be easily described by means of a spatially varying electronic density, or, in other words, by a spatially varying penetration depth. Core pinning is more delicate to model within the London framework, but a core-pinning center could, for example, be modeled by a very large value of the penetration depth in a very small region. Various situations are described in Sec. IV.

III. NUMERICAL TECHNIQUES

Numerically, the problem consists of solving the London equation to calculate the interactions needed to compute the total energy of a configuration of vortices and then to minimize this energy with respect to the positions of the vortices. Since the total energy of the vortex system has to be evaluated frequently, it is important to use a very efficient method to solve the London equation.

In two dimensions, when the vortex cores are aligned along the z axis, $\mathbf{b}(\mathbf{r}, \mathbf{r}') \equiv f(x,y)\hat{\mathbf{z}}$ and Eq. (1) become

$$\frac{\partial}{\partial x}\left[\lambda^2(x,y)\frac{\partial f(x,y)}{\partial x}\right] + \frac{\partial}{\partial y}\left[\lambda^2(x,y)\frac{\partial f(x,y)}{\partial y}\right] + f(x,y) = \delta(\mathbf{r}-\mathbf{r}') \tag{12}$$

which is a standard positive-definite, symmetric, second-order, elliptic partial differential equation whose solution can be obtained by a variety of numerical methods. The first step in obtaining a solution is to discretize the equation, thereby reducing it to a linear system of equations $Af = g$ where the matrix A represents the discretization of the left-hand side, f, the unknown fields at $\mathbf{r} = (x,y)$, and g, the vortex at $\mathbf{r}' = (x',y')$.

There are two general classes of methods to solve this linear system of equations. With direct methods, the matrix A is factorized and f is found by back substitution. For our problem the attractive feature of this class is the need to do the factorization only once at the beginning of the problem: When we change vortex positions, we just change g and find f by back substitution using the previously computed and stored factorization. The unattractive feature of this approach is the often large storage requirements of the factorized matrices, which are, in general, dense matrices even though A is very sparse. The second class of methods includes relaxation methods. With them, the storage requirements are minimal, but their convergence can be slow, leading to significant computation time.

Since we are initially interested in whether the overall computational approach yields physically reasonable results, we decided to reduce the computational complexity by restricting the calculation to one dimension. Here, the direct method of solution is highly attractive. Since A is positive definite, we used Cholesky decomposition[8] to produce $A = LL^T$, where L is a lower-triangular matrix. When we discretized our operator onto M grid points using

$$\frac{d}{dx}\left[\lambda^2(x)\frac{df}{dx}\right] \approx \lambda^2\left[x+\frac{h}{2}\right]\left[\frac{f(x+h)-f(x)}{h}\right] + \lambda^2\left[x-\frac{h}{2}\right]\left[\frac{f(x)-f(x-h)}{h}\right] , \tag{13}$$

we found that L requires only $3M$ elements of storage and

the number of steps in backsubstitution is proportional to M. We chose our discretization parameter h to be about one-tenth of the penetration depth, and since the magnetic field around a vortex decreases on a length scale of λ, we chose our system size to be at least ten times the average spacing between vortices. We assumed periodic boundary conditions.

In one dimension, minimizing $E(\mathbf{r}_1,\mathbf{r}_2,\ldots,\mathbf{r}_N) = E(x_1,x_2,\ldots,x_N)$ with respect to the position of the vortices is mathematically equivalent to minimizing a nonlinear function of N variables. Since we want to treat systems with a reasonably large number of vortices, it is imperative to use a reliable, and hopefully efficient, method to perform the minimization. A wealth of algorithms and methods have appeared in combinatorial optimization in the recent past. We chose to use a simulated annealing method which is a stochastic optimization technique that mimics the metallurgical annealing process.[9] The specific algorithm we use is that of Corana *et al.*[10]

The method is Monte Carlo based. One moves a vortex from $\mathbf{r}\rightarrow\mathbf{r}+\delta\mathbf{r}$, producing a change in the configuration energy ΔE. The change is accepted according to the Metropolis algorithm with probability P,

$$P=\min(R,\ e^{-\Delta E/T}) , \tag{14}$$

where R is a random number uniformly distributed between 0 and 1 and T is a fictitious temperature. The tendency is to accept vortex moves that lower the energy, but there is the possibility of allowing "thermal fluctuations" to "hop" the vortex out of a metastable state. After "annealing" at T for a suitable number of attempted moves over the entire system (a sweep), one repeats the process at successively lower temperatures, always recording the current value and configuration of lowest energy, until the energy converges to a suitable accuracy. In one dimension, the movement $\delta\mathbf{r}$ is a multiple of the grid spacing. Typically, we would sweep 60 times at a given temperature and then reduce the temperature by 70% to move to the next annealing step. We would anneal until the differences in the energies at the end of three successive annealing steps and the current optimal value were within 1 part in 10^{-4} of each other. We used 200 grid points. On a Cray-XMP computer, the calculation took less than 1 min of CPU time, but most calculations were done on scientific work stations. The distinctive feature of our algorithm was the dynamic adjustment of the maximum allowable step size to insure that between 40% and 60% of our moves were accepted.[10] This adjustment promotes the efficient sampling of possible configurations.

Our solution to the London equations yields the fields at each grid point produced by a vortex at a particular point x_i; hence, from it we obtain the interaction between that vortex and all other vortices on the grid. Clearly, one sees that if we move the vortex at x_i, then to find the interactions we have to resolve the London equation with the vortex at this new position. The discretization provides an automatic cutoff length for the vortex self-interaction. The energy expression we minimize is

$$E=\frac{\Phi_0}{\mu_0}\sum_{i\le j}^{N} b_z(x_i,x_j) , \tag{15}$$

where $b_z(x_i,x_i)$ is the self-interaction determined numerically and not by Eq. (11). To compute a pinning force F_p, we minimize[4]

$$E'=E-F_p\sum_{i=1}^{N} x_i . \tag{16}$$

IV. RESULTS

To illustrate our method, we present the results obtained for various spatial distributions of the penetration depth λ. For the simplest variations, for example, a region with different λ embedded in a host, we can solve exactly the differential equation for one vortex and compare this solution with our numerical solution. In all cases, whether the vortex is inside or outside this region, the solutions agree to five or six decimal places. The simplest test of our ability to produce a correct flux-line lattice is to take a perfectly homogeneous system (λ constant), and check that the configuration obtained corresponds to equally spaced flux lines. Starting with a set of eight vortices initially distributed on the grid, we get the field distribution shown in Fig. 1(a) which is indeed the expected regular flux lattice. A somewhat more complex situation is shown in Fig. 1(b). Here, the penetration depth is constant everywhere except in a small region of 33 grid points where λ is twice as large. In order to minimize its self-energy, a flux line would rather move to regions where the penetration depth is large. If we had only one flux line in the system just described, it would sit right in the middle of the small region where λ is largest. This is the generic behavior of an individual flux line. On the other hand, flux lines repel each other, and tend to stay as far away from one another as they can in order to minimize their interaction energy. Each flux line will minimize its self-energy while avoiding the other flux lines which determines the structure of the flux lattice in disordered systems. Hence, it is important to use the exact (long-range) interaction potential between the vortices in order to obtain the correct FLL structure in a disordered medium. The competition between the one- and two-body terms in the total energy of the FLL [Eq. (6)] will be illustrated several times in the remainder of this section. In this situation shown in Fig. 1(b), two vortices (out of a total of eight vortices) are trapped in the central defect. The penetration of more vortices in that region is not advantageous as it would increase the total energy of the system because of the repulsion with the two vortices already present. Notice also that the two vortices trapped in the defect tend to stay as far apart as they can, but they are not necessarily located exactly on the edges of the defect on account of the presence of the other vortices outside the defect. A depression in the penetration depth has the opposite effect. A small λ would increase the self-energy of a vortex which, hence, tends to stay away from such regions. This effect is illustrated in Fig. 1(c), where a region of 33 grid points, the penetration depth is only one-third its value outside the defect. No

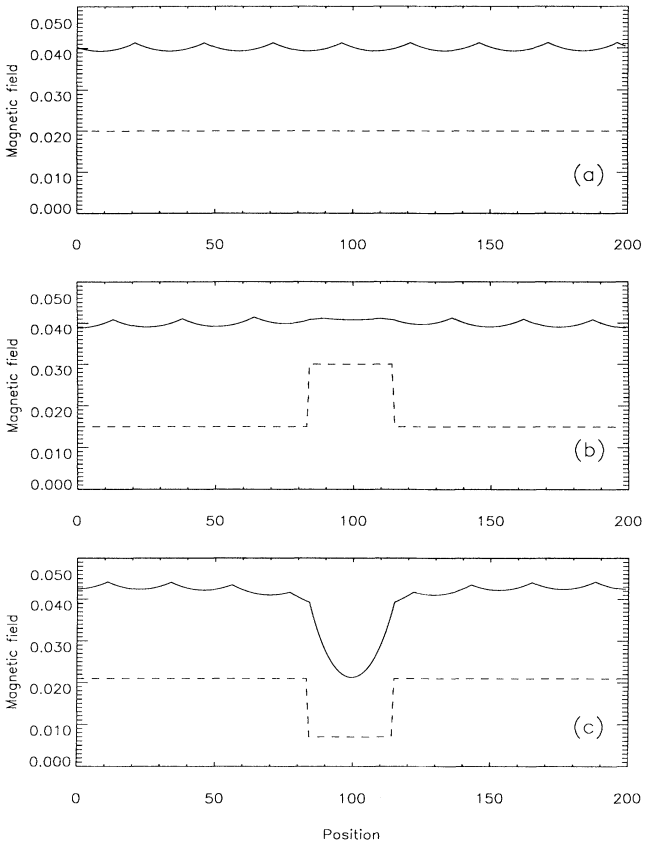

FIG. 1. Various vortex configurations for a system of eight flux lines. The computational grid has 200 equally spaced points separated by a distance of 0.025 λ, where λ is the penetration depth. (a) The penetration depth λ is uniform and the flux lines form a perfect lattice. (b) The value of the penetration depth in a central region 33 grid points wide is twice the outside value. Two flux lines are trapped inside the defect. (c) The value of the penetration depth in a central region 33 grid points wide is one-third the outside value. The flux lines avoid the defect since sitting in that region increases their self-energy.

flux lines penetrate inside the defect. If one were to increase the number of flux lines in the system, the interaction energy would increase, and, at some point, one flux line would penetrate inside the region where λ is smaller. The 'phase diagrams' shown in Figs. 2 and 3 summarize the above discussion. Figure 2 represents the situation where the penetration depth is enhanced inside the defect. The two axes are associated with the two competing terms in Eq. (6). A large defect will give the advantage to the self-energy (one-body) term, whereas a large number of vortices will increase the interaction energy (two-body term). Depending on which term dominates, one, two, three, or more vortices will get trapped by the defect. Figure 3 depicts the situation of a small penetration depth inside the defect and can be interpreted in a similar manner. The energy (for a fixed number of flux lines) is a continuous function of the defect size, but it has a cusp

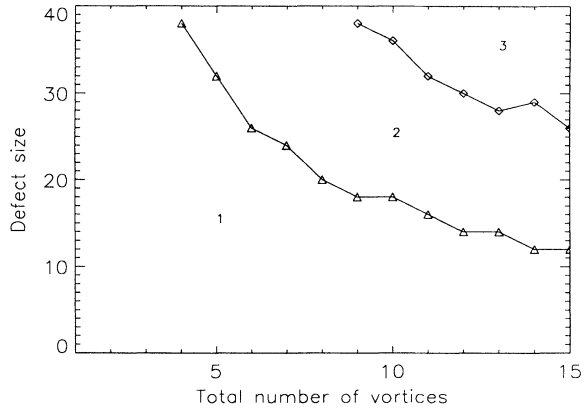

FIG. 2. "Phase diagram" for an attractive defect. The defect is as described in Fig. 1(b). The lines joining the points in the diagram are merely a guide for the eye.

(i.e., a jump in the first derivative) each time the system switches to another phase. This is shown in Fig. 4 for the case where λ is larger inside the defect.

A second, perhaps more interesting, model of the spatial variation of λ corresponds to a random distribution of defects. To be specific, we considered a penetration depth distribution of narrow (two or three grid points) peaks and dips randomly distributed (position and strength) on a grid. Two situations are of interest; first, we considered relatively weak pinning centers. On the whole, one would expect the self-energy term to have a rather small effect on the regularity of the spacing between the flux lines. This is indeed the case as is shown in Fig. 5(a). The effect of the weak pinning centers is simply to move the entire flux structure and lock it in a position where the individual flux lines will be able to minimize their self-energy. Presumably, this means that a few flux lines in the FLL will be found at sites where λ is large. Of course, the regular spacing between the flux

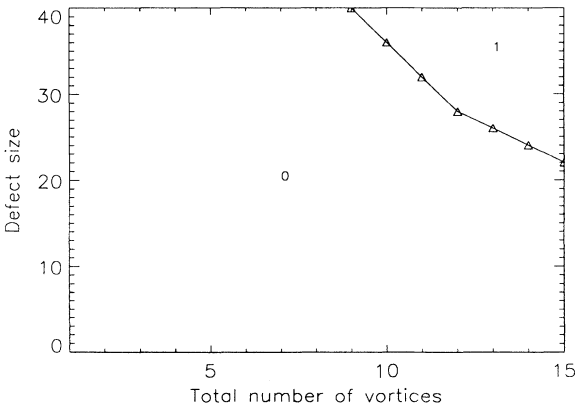

FIG. 3. "Phase diagram" for a repulsive defect. The defect is as described in Fig. 1(c). The lines joining the points in the diagram are merely a guide for the eye.

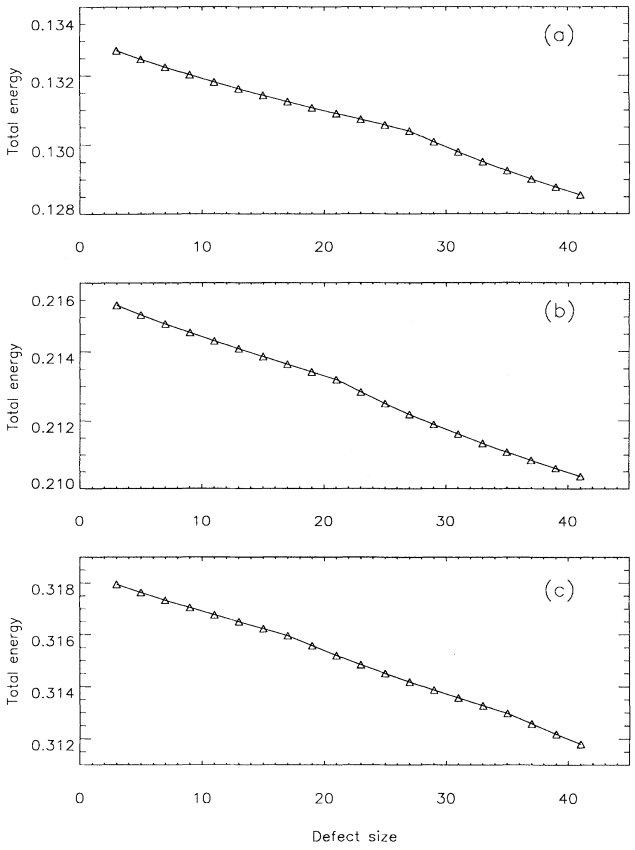

FIG. 4. Total energy of the FLL vs defect size for a system of (a) six vortices, (b) eight vortices, and (c) ten vortices. The defect is as described in Fig. 1(b).

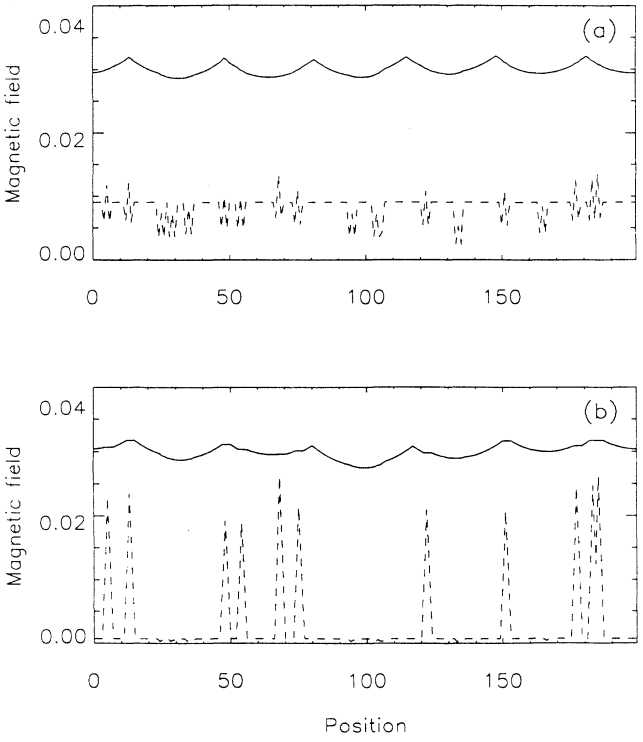

FIG. 5. FLL in a random medium. (a) Weak pinning: The repulsive forces between the vortices dominate, and a short-range ordered flux-lattice structure still exists. (b) Strong pinning. The microstructural configuration of the medium is the same as in (a), but the strength of the pinning sites has been increased by a factor of 5. The FLL is completely disordered, reflecting the disorder of the underlying medium.

lines cannot, strictly speaking, be maintained over large distances, i.e., the *long*-range order is destroyed as predicted by Larkin and Ovchinnikov,[11] but a *short*-range order survives. This is indeed apparent in Fig. 5(b). In the second situation, we considered the case of very strong pinning. Here, the self-energy term dominates, and each individual flux line locates itself to minimize its self-energy, regardless (more or less) of what the other flux lines do. All order in the FLL is lost, and its disordered structure merely reflects the disorder of the underlying material microstructure. As emphasized previously, this order-disorder transition is the result of the competition between the one- and two-body terms in Eq. (6) in the presence of the disordered medium.

One last situation of interest is the application of an external depinning force. As pointed out in the preceding section, using Eq. (16), we can easily account for an average external force acting on each flux line. In Fig. 6(a) we show a FLL when the depinning force $F_p=0$. Two vortices are trapped in the defect. In Fig. 6(b) we applied a depinning force from the left to the right of magnitude $F_p=0.004$. We find that most of the vortices have piled up on the right-hand side of the lattice with one vortex remaining to the left of the defect while two vortices are trapped at the right edge of the defect. In Fig. 6(c) we shown the FLL with F_p has been increased to 0.008. Two vortices remain at the right edge of the defect with the rest pushed up to the right edge of the lattice. With respect to Fig. 6, we remark that some cusp-like features in the magnetic field arise as consequence of the sharp boundaries between the regions of different values of λ and, consequently, are not always indicative of vortex positions. In Fig. 6(c) the applied external force is strong enough to cause two vortices to occupy grid position 200.

We feel these figures show that it is easy to obtain a qualitative picture of the effects of the depinning force. To be quantitative, we remark that we would have to modify the way we do the simulation. With a relatively short chain and periodic conditions, the defects swept to the right edge form a large repulsive cluster which by itself can inhibit the vortices from depinning. For the case of Fig. 6, for example, increasing F_p past 0.008 up to 0.016 produces minor changes in the FLL. One vortex leaves the defect, with the remaining one continuing to be trapped at the rightmost edge. In one-dimension, because the computation time for long chains would not be very significant, this boundary effect can be significantly

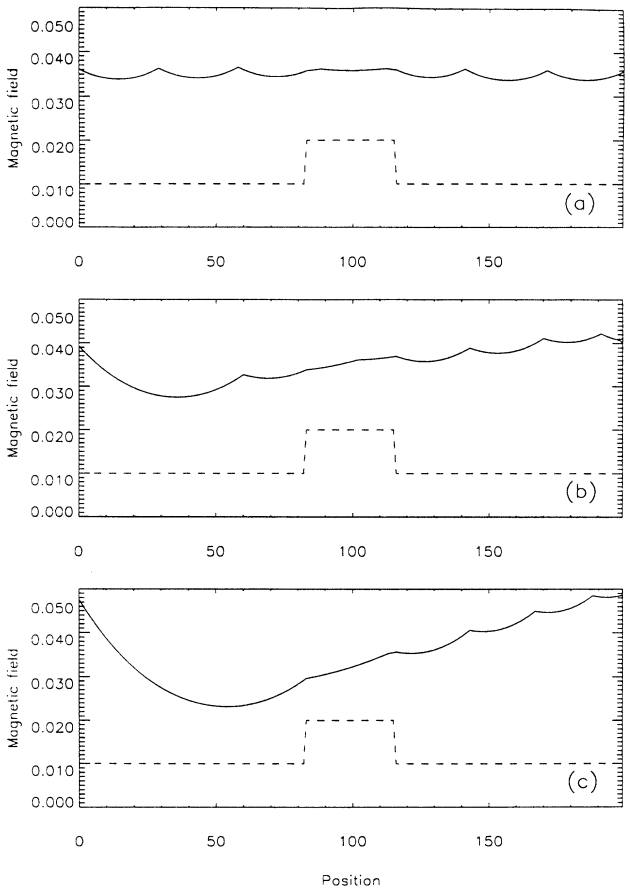

FIG. 6. Vortex depinning. The defect is as described in Fig. 1(b). There are seven vortices and the depinning force is applied left to right. The left and right edges of the defect are at grid positions 83 and 117. (a) $F_p=0$ with two vortices trapped inside the defect. (b) $F_p=0.004$ vortex positions at 61, 103, 117, 144, 171, 192, and 200. (c) $F_p=0.008$ with vortex positions at 114, 117, 144, 168, 189, 200, and 200.

reduced by simply making the chain very long with respect to the defect size. In higher dimensions, this procedure could become impractical, and more careful attention will probably be needed to the consistency of boundary conditions and spatial dependence of the applied external force.

V. CONCLUSIONS

In conclusion, we presented the basic equations that permit the efficient simulation of vortex structures in materials whose superconducting behavior is described by the London equations. We showed that the energy of such structures is the sum of a self-interaction part, which depends on the local variation of the penetration depth, and a sum of pair interactions, which are the Green's function of the London equation for an inhomogeneous material. Within this formalism, the exact (London approximation) long-range interaction between flux lines is used, contrary to previous similar simulations. Also, in contrast to previous simulations, various defects can be modeled in a more realistic way by allowing the penetration depth to vary spatially with the effects of that spatial dependence on the interaction between the flux lines being automatically and exactly taken into account. Additionally, pinning arises in a natural manner instead of being assumed. The equations were solved for a variety of one-dimensional models of inhomogeneities and physically reasonable results were found.

The formalism is general. The case of a two-dimensional flux-line system is currently under study, and the results will be presented elsewhere. The formation of a FLL in a two-dimensional system of vortices and the influence of different types of microstructural defects on the FLL are among the most interesting applications of our method. One important aspect of the problem is the modeling of defects in terms of spatial variations in the electronic density (and, hence, in terms of the penetration depth λ). Few microstructure models are currently available.

Finally, as described, our method was used to determine the (static) equilibrium structural properties of the FLL. For the applications presented here we were only able to calculate equilibrium configurations. How this equilibrium is reached is also an important question for such problems as flux creep, critical states, etc. For these problems, it is easy to write a Langevin equation for the motion of the flux lines. The forces appearing in this equation can be obtained from the formalism described in Sec. II with the use of $\mathbf{F}=\mathbf{j}\times\mathbf{B}$ and $\mathbf{j}=\nabla\times\mathbf{B}$. These forces automatically include the microstructure of the material under consideration. One can then alternate between a calculation of the forces acting on each vortex in the current configuration, and a time step in the integration of the Langevin equation, hereby producing a new set of flux line positions which can then be used to produce a new set of forces, etc. Such a calculation is currently underway.

ACKNOWLEDGMENTS

This work was supported by the U.S. Department of Energy. We gratefully acknowledge helpful conservations with L. Campbell and S. Trugman.

[1]J. R. Cave and J. E. Evetts, J. Low Temp. Phys. **63**, 35 (1986).
[2]Z. Radović, S. Radojev, and L. Dobrosavijecić, J. Low Temp. Phys. **54**, 107 (1984); M. Ledvij, Z. Radović, and L. Dobrosavijecić, *ibid.* **67**, 331 (1987).
[3]L. L. Daemen and J. E. Gubernatis, Phys. Rev. B **43**, 2625 (1991).
[4]E. H. Brandt, J. Low Temp. Phys. **53**, 41 (1983); **53**, 71 (1983).
[5]A. Brass, H. J. Jensen, and A. J. Berlinsky, Phys. Rev. B **39**, 102 (1989); H. J. Jensen, A. Brass, A. C. Shi, and A. J. Berlinsky, *ibid.* **41**, 6394 (1990); H. J. Jensen, A. Brass, Y. Brechet,

and A. J. Berlinsky, Cryogenics **29**, 367 (1989).
[6]P. G. de Gennes, *Superconductivity of Metals and Alloys* (Benjamin, New York, 1966).
[7]R. P. Huebener, *Magnetic Flux Structures in Superconductors* (Springer-Verlag, Berlin, 1979), p. 186.
[8]G. H. Golub and C. F. van Loan, *Matrix Computations* (Johns Hopkins, Baltimore, 1989).
[9]S. Kirkpatrick, C. D. Gelatt, and M. P. Vecchi, Science **220**, 671 (1983).
[10]A. Corana, M. Marchesi, C. Martini, and S. Ridella, ACM Trans. Math. Software **13**, 262 (1987).
[11]A. I. Larkin and Yu. N. Ovchinnikov, J. Low Temp. Phys. **34**, 409 (1979).